View metadata, citation and similar papers at core.ac.uk

brought to you by CORE

provided by National Chung Hsing University Institutional Repository

Angewandte Chemie

Eine Zeitschrift der Gesellschaft Deutscher Chemiker

Supporting Information

© Wiley-VCH 2012

69451 Weinheim, Germany

A Nanoscale Force Probe for Gauging Intermolecular Interactions**

*Minkyu Kim, Chien-Chung Wang, Fabrizio Benedetti, and Piotr E. Marszalek**

anie_201107210_sm_miscellaneous_information.pdf

Constructing a protein-based force probe

The force probe composed of three SNase domains and four I27 domains of titin, pAFM1-8 (SNase 2,4,6), was constructed by replacing each individual module of pAFM1-8 plasmids as previously described.[1-2] The *Strep*-tag II,[3] WSHPQFEK, was synthesized and fused into the position 8 of pAFM 1-8(SNase 2, 4, 6) plasmids. Human RNase inhibitor (RI) gene (residues 1-461, NCBI, NM_203385.1) terminated with the *Strep*-tag II and human angiogenin (ANG) gene (residues 1-147) were also cloned into the position 8 of the pAFM plasmid. Human ANG gene (NCBI, BC054880) was synthesized and cloned into the pUC57 vector by GenScript (Piscataway, NJ, USA). All plasmids were transformed into *E.coli* OverExpress C41(DE3)pLysS cells (Lucigen, Middleton, WI, catalog #60444). A freshly-grown bacterial colony was inoculated in a 3ml LB broth medium with 1mM ampicillin at 37˚C for overnight. For pre-culture, 50µl of overnight culture of I27-(SNase-I27)$_3$-*Strep*-tag II, I27-(SNase-I27)$_3$-RI and I27-(SNase-I27)$_3$-ANG were inoculated into 5ml EB™ (Zymoresearch, Orange, CA, USA, catalog # M3012) for 4 hours at 37˚C (OD_{600} > 1). Proteins were expressed from cultures grown overnight at RT by adding 15ml of OB ™ (Zymoresearch, catalog # M3013) in the presence of 0.5mM IPTG. Cells were harvested by spinning down at 4k x g for 20 min, and then frozen at -80˚C. Thawed cells which contain I27-(SNase-I27)$_3$-*Strep*-tag II, I27-(SNase-I27)$_3$-ANG and I27-(SNase-I27)$_3$-ANG were suspended in a Lysis buffer including Lysozyme and Benzonase Nuclease (QIAGEN, catalog #37900). The buffers contained an additional 10mM Tcep (Thermo Scientific, Rockford, IL, product #77720) to prevent the oxidation of the cysteine residues in the I27-(SNase-I27)$_3$-RI protein during the cell lysis and protein purification steps. This buffer prevents oxidation of RI, which can cause the loss of binding activity to the angiogenin.[4-5] The lysates were spun down at 14k x g for 30 min at 4˚C. All proteins, which contain N-terminal 6x His-tag, were purified using Ni-NTA Superflow Column (QIAGEN, catalog #30622). Then, the I27-

(SNase-I27)$_3$-RI protein was purified by *Strep*-Tactin Sepharose column (IBA GmbH, Göttingen, Germany, catalog #2-1202-051). The I27-(SNase-I27)$_3$-ANG protein was chromatographed using a Superose 12 gel filtration column and a size-exclusion HPLC machine. The I27-(SNase-I27)$_3$-*Strep*-tag II protein was loaded into the Slide-A-Lyzer G2 Dialysis Cassette (Thermo Scientific, Rockford, IL, USA, product #87735) and dialyzed against 2L of 100mM Tris-HCl, 150mM NaCl and 1mM EDTA buffer with the addition of 0.5 mM Tcep (pH ~7.6) for overnight. All proteins were concentrated using Amicon Ultra-0.5 centrifugal filter devices (50 kDa for I27-(SNase-I27)$_3$-*Strep*-tag II and I27-(SNase-I27)$_3$-ANG and 100 kDa for I27-(SNase-I27)$_3$-RI) (Millipore, Billerica, MA, USA, catalog # UFC505024 and UFC510024). The buffer of I27-(SNase-I27)$_3$-ANG and I27-(SNase-I27)$_3$-RI was exchanged to 100 mM MES, 150 mM NaCl, 1mM EDTA and 10mM Tcep buffer (pH ~6)[6] by using the filter devices.

Strep-tag II/_Strep_-Tactin and RNase inhibitor/angiogenin complexes preparation for AFM measurements

To create *Strep*-tag II and *Strep*-Tactin complexes, 1.1 μM of *Strep*-tagged I27-(SNase-I27)$_3$ and 10~100 nM of soluble *Strep*-Tactin (IBA GmbH, Göttingen, Germany, catalog #2-1204-005) were mixed in solution containing 100 mM Tris-HCl (pH 7.6), 150 mM NaCl, 1mM EDTA and 0.5 mM TCEP for more than 30 min at RT. ~30 μM of I27-(SNase-I27)$_3$-ANG and ~30 μM of I27-(SNase-I27)$_3$-RI were pre-incubated with the molar ratio of 1:1 in the buffer containing 100 mM MES, 150 mM NaCl, 1 mM EDTA and 10 mM Tcep for more than 20 min at RT and stored at 4℃. For the control experiment, I27-(SNase-I27)$_3$ proteins were prepared. Prepared samples, the mixture of I27-(SNase-I27)$_3$-*Strep*-tag II and *Strep*-Tactin, the mixture of I27-(SNase-I27)$_3$-ANG and I27-(SNase-I27)$_3$-RI, and the control

sample, were diluted 50-70 times in the buffer containing 100 mM Tris-HCl, 150 mM NaCl, 1 mM EDTA and 10 mM Tcep (pH ~7.4) and then incubated on a freshly cleaned gold surface. After 30 min incubation at RT, all samples, without washing, were utilized for the AFM pulling experiment.

Single molecule AFM measurements

All stretching measurements were carried out on custom-built AFM instruments equipped with an AFM detector head from Veeco Metrology Group (Santa Barbara, CA, USA), and high-resolution piezoelectric stages from Physik Instrumente (PI, Karlsruhe/Palmbach, Germany), equipped with capacitive or strain-gauge position sensors (vertical resolution of 0.1 nm).[7-8] All samples were picked up for measuring the binding interactions or detachment forces with an untreated sharpened microlever AFM cantilevers with 12~19 pN/nm of spring constants (k_c) (MSNL, Veeco, Santa Barbara, CA, USA) or biolever AFM cantilevers with 5~10 pN/nm of k_c (OBL, Veeco, Santa Barbara, CA, USA). The spring constant of each cantilever was calibrated in the same buffers that are used for the sample preparation on a fresh mica substrate using the energy equipartition theorem as described previously.[9] The RMS force noise for the biolever and the microlever was ~5 pN and ~12 pN in the 1-500 Hz bandwidth, respectively.

Identifying rupture events of individual biomolecular pairs

When *Strep*-tagged force probes are connected to the *Strep*-Tactin, several possible pulling geometries can be generated because each *Strep*-Tactin may have from zero up to four force probe molecules attached to it (Figure S1). To identify force-extension curves of individual molecular pairs, we established following selection criteria. Four up to six

regularly spaced SNase unfolding force peaks need to be recorded to ascertain that two *Strep*-tagged force probes/*Strep*-Tactin bonds connected *in series* were subjected to the applied force via handles (Figure 1a and Figure S1a). These SNase force peaks should be similar to the force peaks produced by SNase domains in control AFM experiments performed on the force probe alone (Figure 1c in the main text and Figure S3). If multiple *Strep*-tag II/*Strep*-Tactin complexes attached *in parallel* are subjected to stretching forces, the unfolding force peaks of SNase are expected to be higher and not regularly spaced as compared to those produced by measurements on single molecules (Figure S1b-d and S2).

Dynamic force spectroscopy of the *Strep*-Tactin/*Strep*-tag II complex

In general, the rupture force of a ligand-receptor system depends on the loading rate.[10-16] We examined this dependence for individual *Strep*-Tag II/*Strep*-Tactin complexes in Figure S5a. We show the distributions of rupture forces at loading rates varying between 50 pN/s and 7000 pN/s. These distributions need to be fitted with two Gaussians rather than one. Following the approach developed by Evans and Ritchie[11] and modified by Hiterdorfer et al.[14], we separately determined the average rupture force, $<F_{\text{rupture-low}}>$ and $<F_{\text{rupture-high}}>$, from the two Gaussian fittings used for each pdf and plotted their dependence on the logarithm of the apparent loading rate (Figure S5). Similar to streptavidin-biotin complexes,[16] we found two linear regions with different slopes for both relationships. We conclude that in the range of examined loading rates, there are two energy barriers[11, 16] between the bound and unbound states for each rupture pathways of the *Strep*-tag II/*Strep*-Tactin complex (see AFM data analysis for the calculation of the kinetic data).

Detailed discussion on two distinct unbinding pathways of the *Strep*-tag II/*Strep*-Tactin complex

To distinguish the origin of two distinct rupture pathways in the *Strep*-Tactin/*Strep*-tag II complex (Figure S5), we examined the structure of the *Strep*-tag II/*Strep*-Tactin complex. *Strep*-Tactin, an engineered version of streptavidin with an increased binding affinity to the *Strep*-tag II, is, like streptavidin, composed of 4 identical monomers, and their internal interfaces are similar to those of streptavidin.[17-19] *Strep*-Tactin monomers tightly bind to each other forming dimers (yellow/blue and brown/green dimers in Figure S6d) which then assemble into tetramers. The large interface (~16 nm^2) between two monomers within one dimer involves seventeen hydrogen bonds (H-bonds) and other non-covalent interactions. This interface is expected to be mechanically strong. The interface between two dimers (yellow-blue dimer and brown-green dimer in Figure S6d) is small (contact area, ~10 nm^2), mediated by relatively weak interactions and only four H-bonds.[19]

A single *Strep*-tag II binds to a *Strep*-Tactin monomer with the dissociation constant (K_D) of ~ 1 μM.[20-21] The binding of a single *Strep*-tag II to a *Strep*-Tactin monomer is mainly attributed to: a salt bridge formed between the side chains of Glu8 of *Strep*-tag II and R84 of the *Strep*-Tactin monomer and hydrophobic interactions between the side chains of P5 of *Strep*-tag II and Y43, Y54 and W79 in the *Strep*-Tactin monomer.[20] The analysis of the crystal structure of the whole complex (PDB:1KL5), shows that there could also be a π-stacking interaction[22-23] involving the side chain of F7 of *Strep*-tag II and the side chain of W120 from another monomer, belonging in the other dimer of *Strep*-Tactin (Figure S6e).

We hypothesize that different pulling geometries and molecular configurations (Figure S6) are responsible for two unbinding pathways of the *Strep*-tag II/*Strep*-Tactin complex. Based on the crystal structure analysis of the *Strep*-tag II/*Strep*-Tactin complex (above), we

hypothesize that high rupture forces, $<F_{rupture\text{-}high}>$, occur when *Strep*-tag ligands are forced to unbind from monomers belonging to one *Strep*-Tactin dimer (Figure S6a; the first rupture pathway). In this scenario, the large and strong interface between the monomers is mechanically rigid and does not yield to applied forces; the mechanically weakest points are located within the *Strep*-tag binding pockets. We further hypothesize that the small rupture forces, $<F_{rupture\text{-}low}>$, occur when *Strep*-tags are bound to monomers belonging to two different dimers (Figure S6b-c; the second rupture pathway). Based on the crystal structure, we speculate that applied torques will reorient the small and weak dimer-dimer interface. The conformational change may result in a movement of W120 of the *Strep*-Tactin monomer (the blue monomer in Figure S6e) away from the F7 of *Strep*-tag II weakening the binding between *Strep*-Tactin and *Strep*-tag II. The importance of W120 has been already reported by experimental observations on streptavidin/biotin complexes. A single point mutant W120F of streptavidin reduces the binding affinity of biotins by six orders of magnitude and shortens the dissociative half-life time from 35h to 0.5h.[24-25] The mechanical significance of W120 in *Strep*-Tactin can similarly be tested in future AFM measurement of W120F *Strep*-Tactin mutants. Further studies involving molecular dynamic simulations of the wild type and mutant *Strep*-Tactin and *Strep*-tag II complexes will help to verify these hypotheses.

AFM data analysis

Probability density functions (pdf) of obtained rupture forces were generated by Gaussian kernel density estimation (KDE)[26] using custom-written codes in Python (Figure 1d and 3c, Figure S4, S5 and S8). By applying Gaussian fits on pdfs, $<F_{rupture}>$ in each apparent loading rate was determined (Figure S5).

The apparent loading rate (dF/dt) was calculated by multiplying constant speed of piezo travelling distances ($v_p=dz_p/dt$) and the effective spring constant (k_{eff}) which count on the

effect of both cantilever and flexible chain linkers of I27-(SNase-I27)$_3$-*Strep*-tag II.[10-11, 14] Effective spring constants were determined by applying linear slope (dF/dz_p) right before the rupture event occurred on the force-piezo travel distance curve as described elsewhere (Figure S7).[14]

To obtain kinetic values for the binding energy profile to the reaction between *Strep*-tag II and *Strep*-Tactin, $\langle F_{rupture} \rangle$ were plotted against the logarithm of apparent loading rates (r) (Figure S5b).[11] The zero strength kinetic off-rate, $k_{off}(0)$, was calculated by the extrapolation of linear slope on the $\langle F_{rupture} \rangle$ - ln(r) plot with the following equation[10-11, 16]:

$$k_{off}(0) = \frac{x_{rupture} \times r_{\langle F_{rupture} \rangle = 0}}{k_B T}$$

where $x_{rupture}$ is the characteristic length scale which represent the distance between bound state to the transition state in the energy profile. From the upper curve in Figure S5b (solid line), we determined $x_{rupture}$ to be ~0.44 nm and ~0.21nm, and $k_{off}(0)$ to be ~0.12 s^{-1} and ~1.21 s^{-1} for outer barrier and inner barrier, respectively. On the other hand, from the lower curve (dashed line), we obtained $x_{rupture}$ to be ~0.51 nm and ~0.24 nm, and $k_{off}(0)$ to be ~0.47 s^{-1} and ~4.83 s^{-1} for outer and inner barriers.

References

[1] A. Steward, J. L. Toca-Herrera, J. Clarke, *Protein Sci.* **2002**, *11*, 2179-2183.
[2] C.-C. Wang, T.-Y. Tsong, Y.-H. Hsu, P. E. Marszalek, *Biophys. J.* **2011**, *100*, 1094-1099.
[3] T. G. M. Schmidt, J. Koepke, R. Frank, A. Skerra, *J. Mol. Biol.* **1996**, *255*, 753-766.
[4] J. Siurkus, P. Neubauer, *Microb Cell Fact* **2011**, *10*.
[5] K. A. Dickson, M. C. Haigis, R. T. Raines, *Prog. Nucleic Acid Re.* **2005**, *80*, 349-374.
[6] F. S. Lee, D. S. Auld, B. L. Vallee, *Biochemistry* **1989**, *28*, 219-224.
[7] A. F. Oberhauser, P. E. Marszalek, H. P. Erickson, J. M. Fernandez, *Nature* **1998**, *393*, 181-185.
[8] P. E. Marszalek, A. F. Oberhauser, Y. P. Pang, J. M. Fernandez, *Nature* **1998**, *396*, 661-664.
[9] E. L. Florin, M. Rief, H. Lehmann, M. Ludwig, C. Dornmair, V. T. Moy, H. E. Gaub, *Biosens. Bioelectron.* **1995**, *10*, 895-901.
[10] G. I. Bell, *Science* **1978**, *200*, 618-627.

[11] E. Evans, K. Ritchie, *Biophys. J.* **1997**, *72*, 1541-1555.
[12] J. Zlatanova, S. M. Lindsay, S. H. Leuba, *Prog. Biophys. Mol. Bio.* **2000**, *74*, 37-61.
[13] P. Hinterdorfer, Y. F. Dufrene, *Nat. Methods* **2006**, *3*, 347-355.
[14] P. Hinterdorfer, A. Ebner, H. Gruber, R. Kapon, Z. Reich, in *Handbook of Nanotechnology*, 3rd ed. (Ed.: B. Bhushan), Springer, **2010**, pp. 763-785.
[15] V. Dupres, C. Verbelen, Y. F. Dufrene, *Biomaterials* **2007**, *28*, 2393-2402.
[16] R. Merkel, P. Nassoy, A. Leung, K. Ritchie, E. Evans, *Nature* **1999**, *397*, 50-53.
[17] W. A. Hendrickson, A. Pahler, J. L. Smith, Y. Satow, E. A. Merritt, R. P. Phizackerley, *P. Natl. Acad. Sci. USA* **1989**, *86*, 2190-2194.
[18] P. C. Weber, D. H. Ohlendorf, J. J. Wendoloski, F. R. Salemme, *Science* **1989**, *243*, 85-88.
[19] S. C. Wu, S. L. Wong, *J. Biol. Chem.* **2005**, *280*, 23225-23231.
[20] I. P. Korndorfer, A. Skerra, *Protein Sci.* **2002**, *11*, 883-893.
[21] S. Voss, A. Skerra, *Protein Eng.* **1997**, *10*, 975-982.
[22] M. J. Betts, R. B. Russell, in *Bioinformatics for Geneticists* (Eds.: M. R. Barnes, I. C. Gray), Wiley, **2003**, pp. 289-316.
[23] A. K. Rappe, G. B. McGaughey, M. Gagne, *J. Biol. Chem.* **1998**, *273*, 15458-15463.
[24] T. Sano, C. R. Cantor, *P. Natl. Acad. Sci. USA* **1995**, *92*, 3180-3184.
[25] A. Chilkoti, P. S. Stayton, *J. Am. Chem. Soc.* **1995**, *117*, 10622-10628.
[26] D. W. Scott, *Multivariate Density Estimation: Theory, Practice, and Visualization*, John Wiley & Sons, Inc., New York, **1992**.
[27] C. Bustamante, J. F. Marko, E. D. Siggia, S. Smith, *Science* **1994**, *265*, 1599-1600.

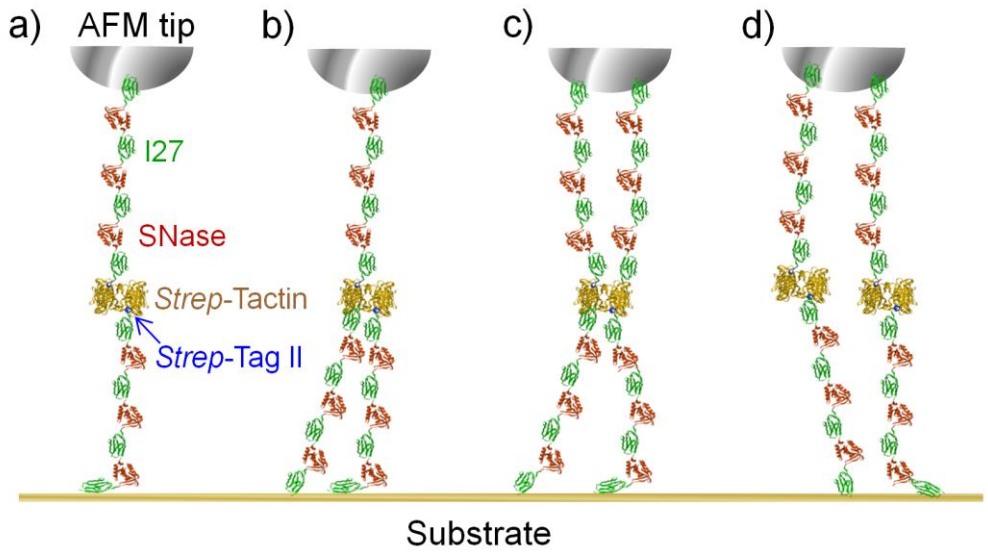

Figure S1. Some possible molecular arrangements between the AFM tip and substrate in force spectroscopy measurements of *Strep*-tag II and *Strep*-Tactin using our I27-SNase based force probe.

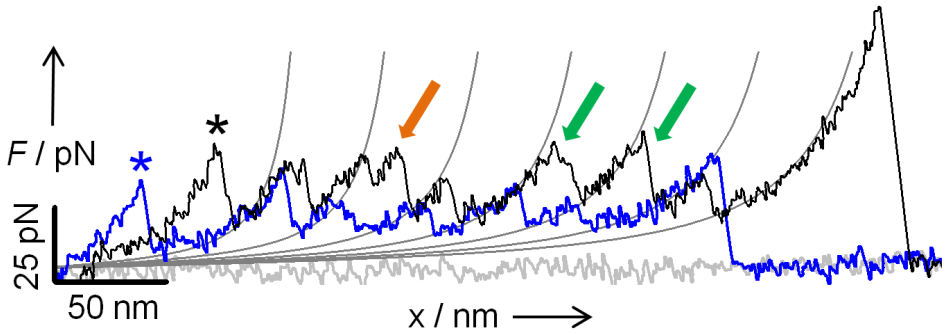

Figure S2. An example of AFM-obtained force-extension curves of individual (blue) versus multiple (black) *Strep*-tagged force probes/*Strep*-Tactin complexes. An addtional unfolding force peak (orange arrow) and higher unfolding force peaks (orange and green arrows) are observed on the black curve. Multiple gray lines are worm-like chain (WLC)[27] model fits to the blue curve with fixed persistent length of 0.9 nm and contour length increment of 47 nm which indicate that the length of the unfolding polypeptide chain is consistent with the structure of SNase.[2] Blue and black star symbols denote a rupture of a nonspecific adhesion bond. Force-extension curves were obtained with the biolever AFM cantilever at the pulling speed of 200 nm/s.

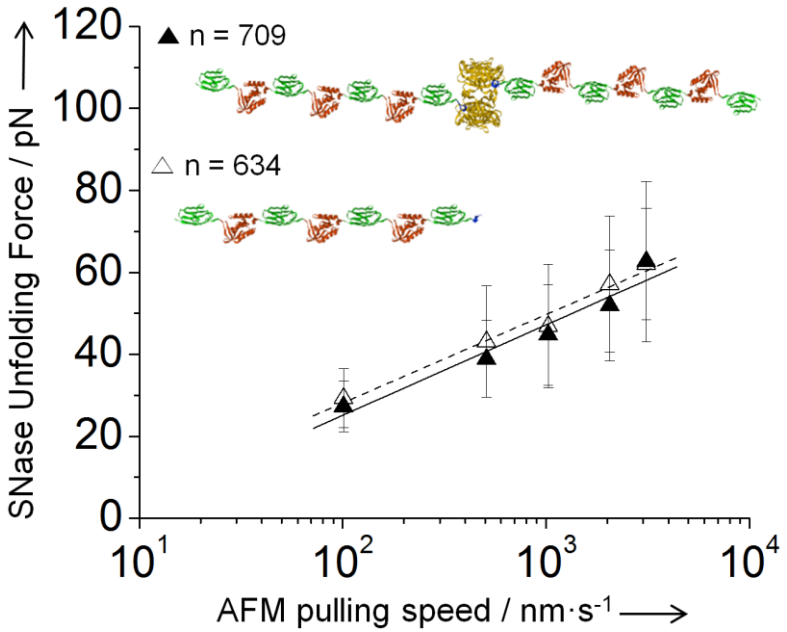

Figure S3. Comparison of average SNase unfolding forces which obtained from *Strep*-tagged force probes/*Strep*-Tactin complexes (filled triangle, solid line) and from force probes alone (empty triangle, dashed line). Error bars represent standard deviation. Data were collected with the microlever AFM cantilever.

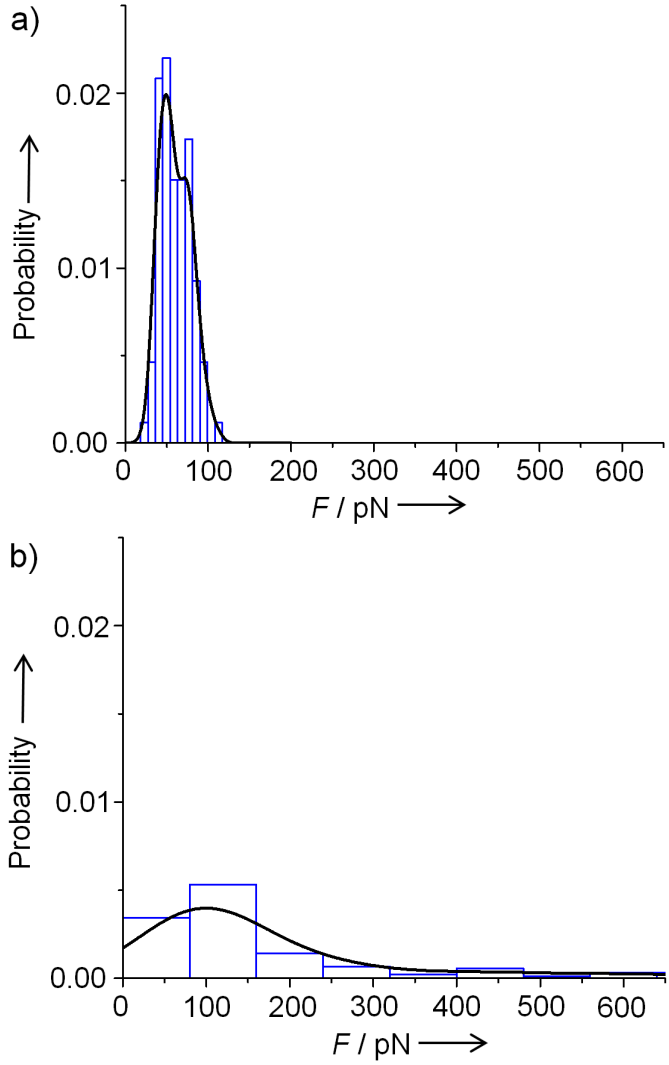

Figure S4. Normalized probability distribution of the last force peaks from *Strep*-tagged force probes/*Strep*-Tactin complexes (a) and force probes alone (b). Black solid curves represent pdfs estimated by Gaussian KDE in this figure and Figure S5a and S8. The histograms are normalized in such a mannor that the total area is equal to 1 in this figure and S8. Data were collected with the microlever AFM cantilever at the pulling speed of 1000 nm/s.

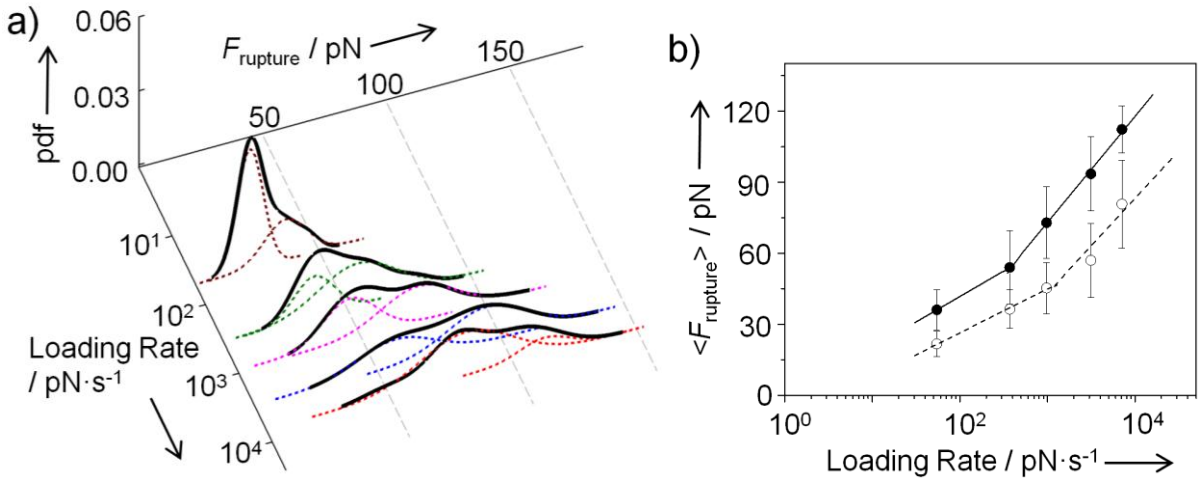

Figure S5. Dependence of *Strep*-tag II/*Strep*-Tactin rupture forces on the loading rates. a) Distributions of rupture forces ($F_{rupture}$) of *Strep*-tag II/*Strep*-Tactin complexes are described by pdfs and various apparent loading rates (black solid curves, n=219). Two Gaussians are applied onto each pdf to determine average rupture forces, $<F_{rupture}>$, in given loading rates. b) $<F_{rupture}>$ from both Gaussian fits (circles ± error bars = mean ± standard deviation) are plotted against the logarithm of apparent loading rates show two linear regions with different slopes for each curve. Filled circles mark $<F_{rupture\text{-}high}>$ and open circles mark $<F_{rupture\text{-}low}>$. Error bars represent standard deviation.

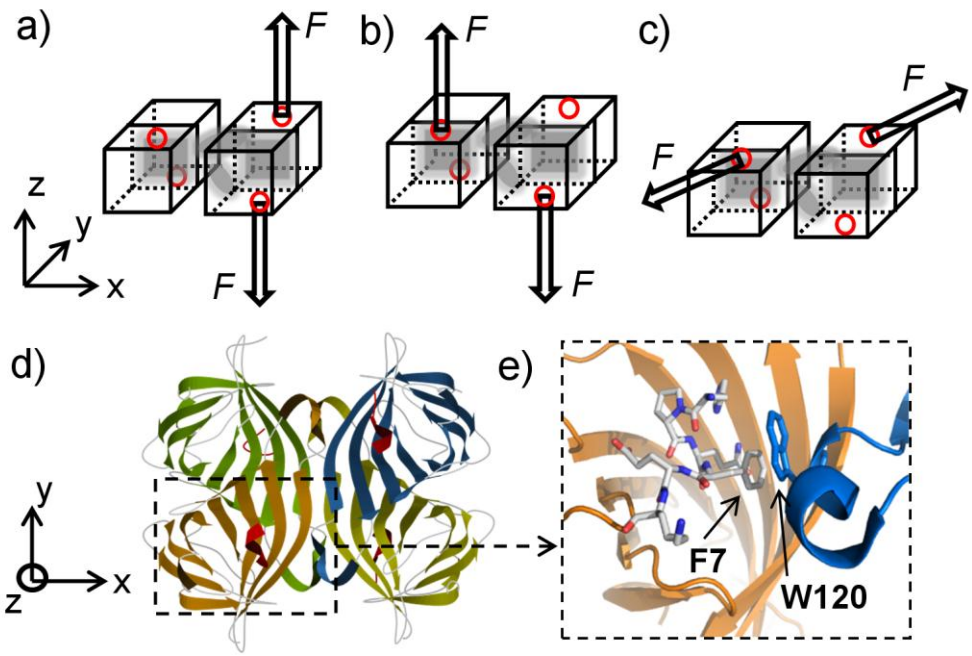

Figure S6. Possible AFM pulling geometries on the *Strep*-tag II/*Strep*-Tactin complex. a) External forces are applied to two monomers within one dimer. Red circles on *Strep*-Tactin indicated *Strep*-tag II binding locations. b-c) External forces are applied to monomers belonging to two different dimers. Gray shades in (a)-(c) represent contact areas between monomers by H-bonds and/or non-covalent interactions. d-e) A schematic of the interface between two dimers (green-brown dimer and blue-yellow dimer) showing a π-stacking interaction[23] between the side chain F7 of *Strep*-tag II (ball and stick model in (e)) and the side chain W120 from the monomer (blue) belonging to the other dimer of *Strep*-Tactin.

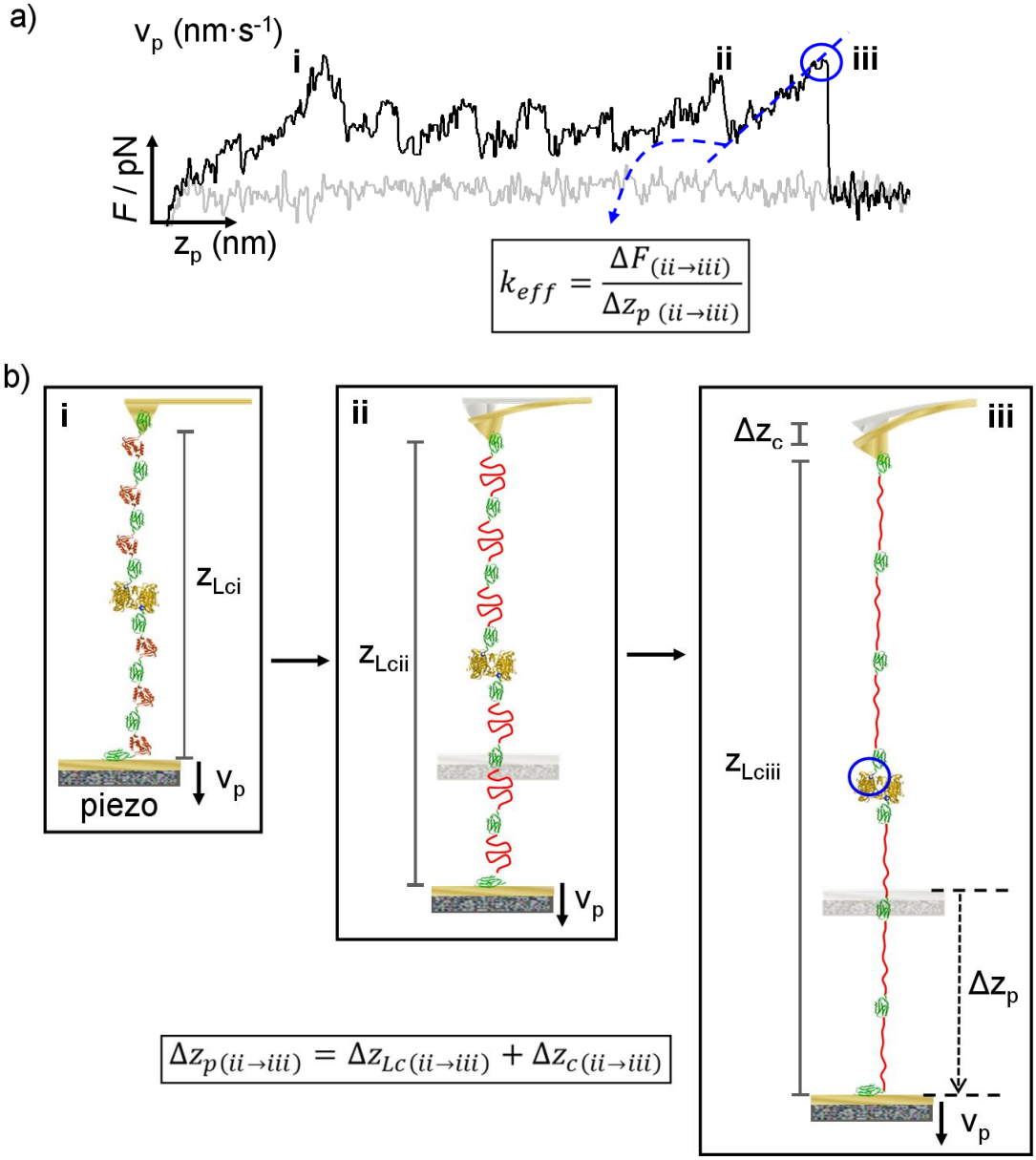

Figure S7. Determination of effective spring constant (k_{eff}) and apparent loading rate (r). a) By measuring the linear slope (ii → iii; dashed blue line) on the curve of force (*F*) - piezo travelling distance (z_p), effective spring constant (k_{eff}), which considered the effect of the cantilever spring constant and the molecular force probes, can be calculated.[14] b) A constant pulling speed applied onto the piezo, v_p, generates external forces onto both AFM cantilever and the protein-based force probes. This causes cantilever bending, Δz_c, and contour length increments on the molecule, $\Delta z_{Lc(ii \rightarrow iii)}$. With obtained values, apparent loading rates can be calculated by the following equation: $r_{App} = k_{eff} \cdot v_p = (\Delta F / \Delta z_p) \cdot (\Delta z_p / \Delta t) = \Delta F / \Delta t$.

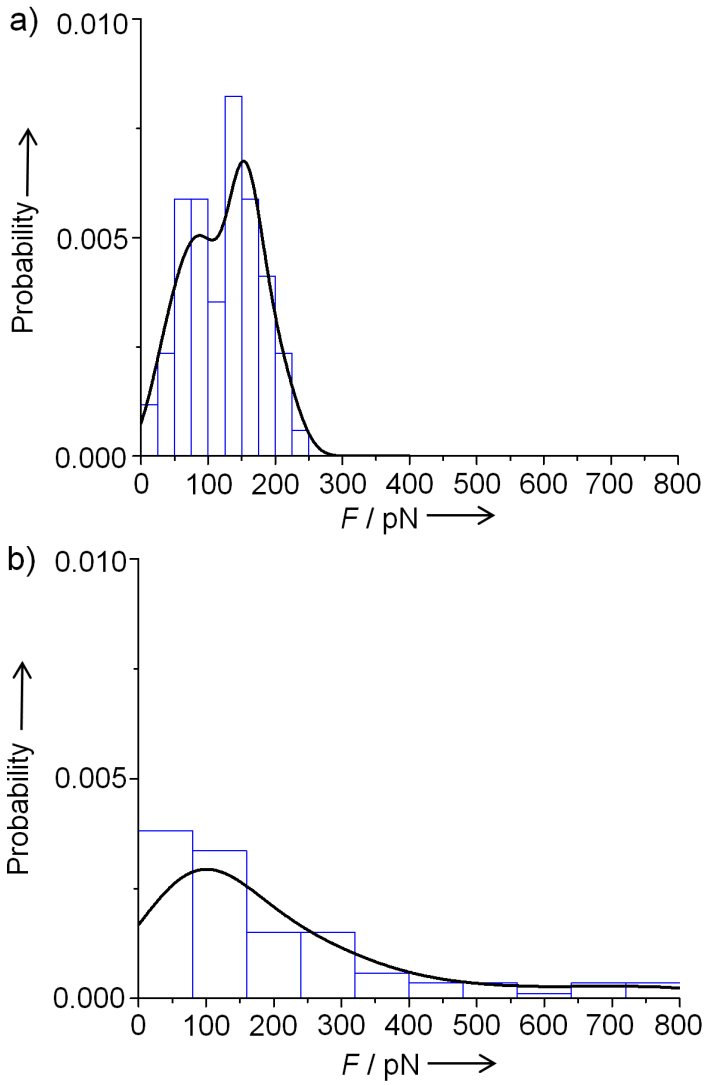

Figure S8. Normalized probability distribution of the last force peaks from RNase inhibitor / angiogenin complexes linked to force probes (a) and force probes alone (b). Data were collected with the microlever AFM cantilever at the pulling speed of 500 nm/s.